# Terrestrial Laser Scanning for the Documentation of Heritage Tunnels: An Error Analysis

**Chris PAGE, Pascal SIRGUEY, Richard HEMI, Ghyslain FERRE, , Elisabeth SIMONETTO, Christophe CHARLET, and Damien HOUVET, New Zealand & France**

**Key Words:** LiDARRAS, Terrestrial Laser Scanning (TLS), Georeferencing, Heritage Documentation, Error Analysis

## SUMMARY

With advancements in Terrestrial Laser Scanning (TLS) technology, it is possible to capture precise 3-Dimensional (3D) point cloud data at up to a million points per second. Each point is assigned 3D coordinates relative to the scan stations origin, a return intensity value, and RGB colouring using internal or external photographic imaging. This paper reports on an analysis of the point cloud accuracy of the LiDARRAS project that scanned the Ronville underground network of quarries and tunnels in Arras, France. The network consists of a series of thousand-year-old chalk quarries linked together by tunnels excavated by the New Zealand Engineering Tunnelling Company during WWI in anticipation of the Battle of Arras on 9 April 1917.

An initial test to assess the accuracy of point cloud data and inform about the configuration of a suitable georeferencing network was completed at the National School of Surveying, New Zealand, prior to fieldwork undertaken in France. Various registration and georeferencing scenarios were tested, providing a framework to undertake the TLS survey in France. The tests show that the geometry of the Ground Control Points (GCPs) network affects more the accuracy of the point cloud than the amount of GCPs being used. Optimising the spatial coverage of GCPs highlights that there may be little difference in accuracy using a different number of GCPs. Additional control scenarios based on the network of GCPs surveyed in the Ronville Sector show that the LiDARRAS scanning project achieved centimetre accuracy despite the challenging underground setting.

Terrestrial Laser Scanning for the Documentation of Heritage Tunnels: An Error Analysis (8891)
Christopher Page, Pascal Sirguey, Richard Hemi (New Zealand), Ghyslain Ferrè, Elisabeth Simonetto, Christophe Charlet and Damien Houvet (France)

FIG Working Week 2017
Surveying the world of tomorrow - From digitalisation to augmented reality
Helsinki, Finland, May 29–June 2, 2017

# Terrestrial Laser Scanning for the Documentation of Heritage Tunnels: An Error Analysis

**Chris PAGE, Pascal SIRGUEY, Richard HEMI, Ghyslain FERRE, , Elisabeth SIMONETTO, Christophe CHARLET, and Damien HOUVET, New Zealand & France**

## 1. INTRODUCTION

Terrestrial Laser Scanning (TLS) has become popular for the documentation of heritage and archaeological sites, monitoring of tunnel deformation, geotechnical applications such as landslide monitoring or rockmass characterisation, and engineering as-built surveys (Nuttens *et al*, 2010; Rodríguez-Gonzálvez *et al*, 2015; Remondino, 2011). Documentation of heritage and archaeological sites is particularly important as those may be subject to ruin due to natural degradation, human induced erosion, and natural disasters. TLS allows heritage sites to be preserved digitally in high detail so as to facilitate conservation or planning and allow appropriate management strategies (Nettley *et al*, 2011).

TLS projects collect point cloud data that can account for millions to billions of points depending on the scanning resolution and number of scan stations. Each measured point has 3D coordinates as well as return intensity value. Internal or external cameras may supplement each point with an RGB value for photo-realistic colouring. 3D data collected by TLS are initially referenced with respect to each station's local coordinate system referred to as the Intrinsic Reference System (IRS). Individual scans are then registered with each other in terms of the IRS of a single scan. Finally, the registered point cloud can be georeferenced in terms of a real world coordinate system, reffered to as the Ground Reference System (GRS) (Bornaz *et al*, 2002; Alba and Scaioni, 2007). Although TLS can be inherently accurate, the registration and georeferencement of numerous scans is exposed to error propagation that can be exagerated in challenging environments such as underground surveys.

This issue is particularly relevant to the LiDARRAS project which involves scanning of the Ronville underground network of thousand-year-old chalk quarries linked together by tunnels excavated by the New Zealand Engineering Tunnelling Company during WWI in anticipation of the Battle of Arras on 9 April 1917. This research documents and compares contrasting error budgets/propagation associated with various TLS survey scenarios applied to scans of a test area at the National School of Surveying, New Zealand, as well as on those of the Ronville sector.

## 2. REGISTRATION AND GEOREFERENCING

Scan registration refers to the process of coordinating all scans relative to a single one treated as a "reference scan", whereas georeferencing refers to transforming the IRS to a GRS. There are several ways of completing the processes of registration and georeferencing, which will be explained in this section, highlighting errors inherent with each step.

## 2.1 Registration

More than one scan may be required to sample complex or large sites. Each scan needs to be transformed into a common reference system using a process known as registration (Lichti and Skaloud, 2010). In TLS the process of registration can be completed by the use of common targets in each scan or using the surface to surface cloud registration method, which relies on sufficient overlap (+30%) between adjacent scans (Bornaz, 2003). A 3D rigid-body transformation is applied to each scan relative to a single reference station. This involves six parameters; namely three rotations and three translations. A scale parameter is not included, given that the scanning instrument is designed to measure "absolute" distances. At least three conjugate points in each scan are required to determine the six parameters. If a scale difference is believed to be present, a 3D similarity transformation may be applied instead of the rigid-body transformation (Lichti and Skaloud, 2010).

Table 1 summarises advantages and limits between the target-based and surface to surface based registration methods. Target-based registration consists in registering successive scans together via the use of common markers acting as tie points in overlapping areas (Fan *et al*, 2015). These markers can be in the form of spheres or checkered targets; paddleboard or paper targets. (Becerik-Gerber *et al*, 2011) as well as cylindrical targets. Bercerik-Gerber *et al* (2011) show that target-based registration with spheres has the highest accuracies due to perfect symmetry from any scanning direction.

**Table 1. Comparison between the target-based registration method and surface to surface registration method.**

| Registration Technique | Method | Advantages | Disadvantages |
|---|---|---|---|
| Common Markers or Target-based | – 3 or more common markers seen in subsequent scans. (In the form of spheres, checkered, or cylindrical targets) | – Can pick discrete points between scans. | – Increased time required placing markers.<br>– Stability of markers.<br>– Post-processing segmentation. |
| Surface to Surface | – Point cloud overlap (30%+ recommended Bornaz, 2003). | – Reduced fieldwork time.<br>– No need for 3 markers to be seen per scan. | – Potential for failed registration without enough overlap. |

The surface to surface registration method relies on sufficient overlap between adjacent scans (Bornaz *et al*, 2003). This type of registration is known broadly as the Iterative Closest Point (ICP) method, proposed by Besl and McKay (1992) whereby a rough alignment between scans is refined iteratively to minimize the average distance between points. Several improvements have been made to enhance the algorithms success rates (Chen and Medioni, 1992; Bae and Lichti, 2008; Theiler

and Schindler, 2012). A disadvantage to this technique is the reliance on the overlap between scan stations. Bornaz *et al* (2003) suggest that discrepancies between common points in subsequent scans can be up to 180mm without sufficient overlap. This approach requires the user to identify common features between the scan stations that will allow the registration process to be completed.

In our case, the placement of targets in France would have been time intensive (~1,000 scans were completed) and the loose gravel surface in certain areas of the tunnels could have compromised the position of spheres, and hence the quality of the registration process. For these reasons, surface to surface registration is used in our work.

## 2.2 Georeferencing

Georeferencing is the process of taking the registered point cloud coordinated in the IRS and aligning it with a real world coordinate system or Ground Reference System (GRS). Georeferencing is important when combining multi-temporal datasets as well as datasets acquired from various techniques (Fan *et al*, 2015). The two common ways of georeferencing point cloud data are the direct and indirect methods (Lichti *et al*, 2005; Pejić, 2013).

Direct georeferencing relies on the scanner being placed over a series of points with known GRS coordinates determined using traditional survey techniques such as a total station or a GNSS receiver (Reshetyuk, 2009 & 2010; Paffenholz *et al* 2010).

Indirect georeferencing uses coordinated markers to georeference the point cloud data. This process involves establishing a network of ground control points (GCPs) to be captured by the TLS instrument, a process that can be time consuming. Reshetyuk (2010) and Becerik-Gerber (2011) argued that the placement of markers can significantly affect the accuracy of the georeferencing process. Understanding the results of a "poor" target configuration versus a spatially "strong" target configuration was important prior to undertaking the fieldwork in France. The following section will highlight the differences found between varying spatial configurations of target placement and the effects on the point cloud accuracies.

## 3. DATA AND METHODS

The previous section described various ways of registering and georeferencing point cloud data. This section presents the methodology used to assess the accuracy of a TLS survey completed at the School of Surveying (SoS), University of Otago, prior to undertaking the fieldwork in the Ronville tunnels, France.

### 3.1 School of Surveying Control Network

Initial accuracy assessments of TLS scenarios were performed at the SoS ground floor (Figure 1) to prepare and inform the survey of the Ronville underground network in France. 41 targets were placed throughout the scan scene, including 5 spheres and 36 checkered targets. Each target was coordinated using a Trimble M3 total station and a least squares adjustment.
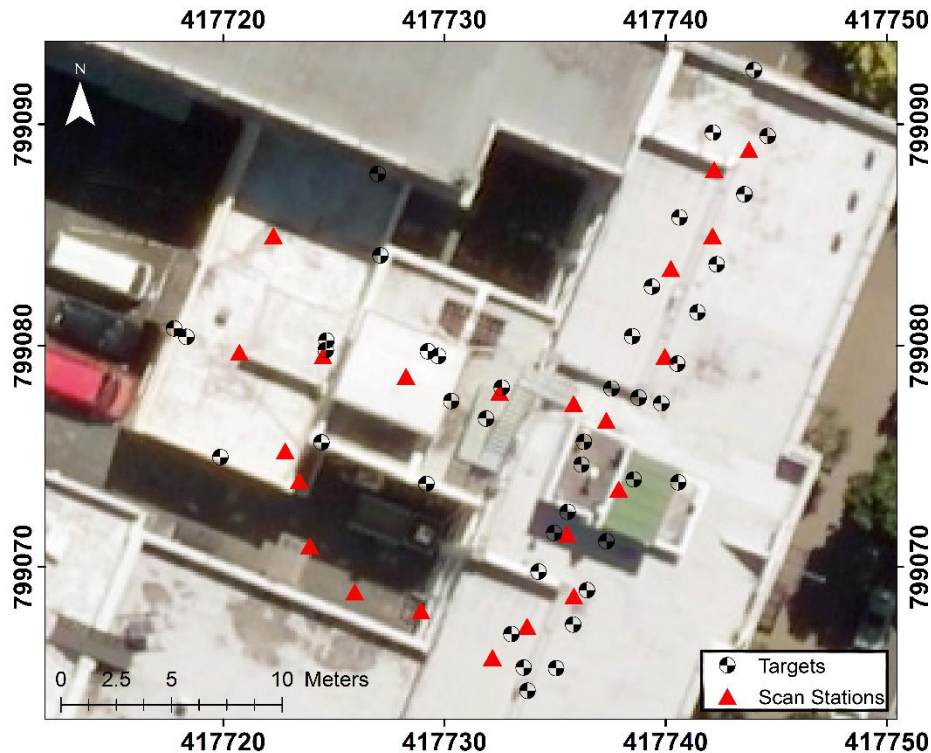
**Figure 1. Test area at the SoS, showing scan stations (triangles) and the horizontal positions of the targets used for each accuracy assessment. Axes represent planimetric coordinates in meters.**
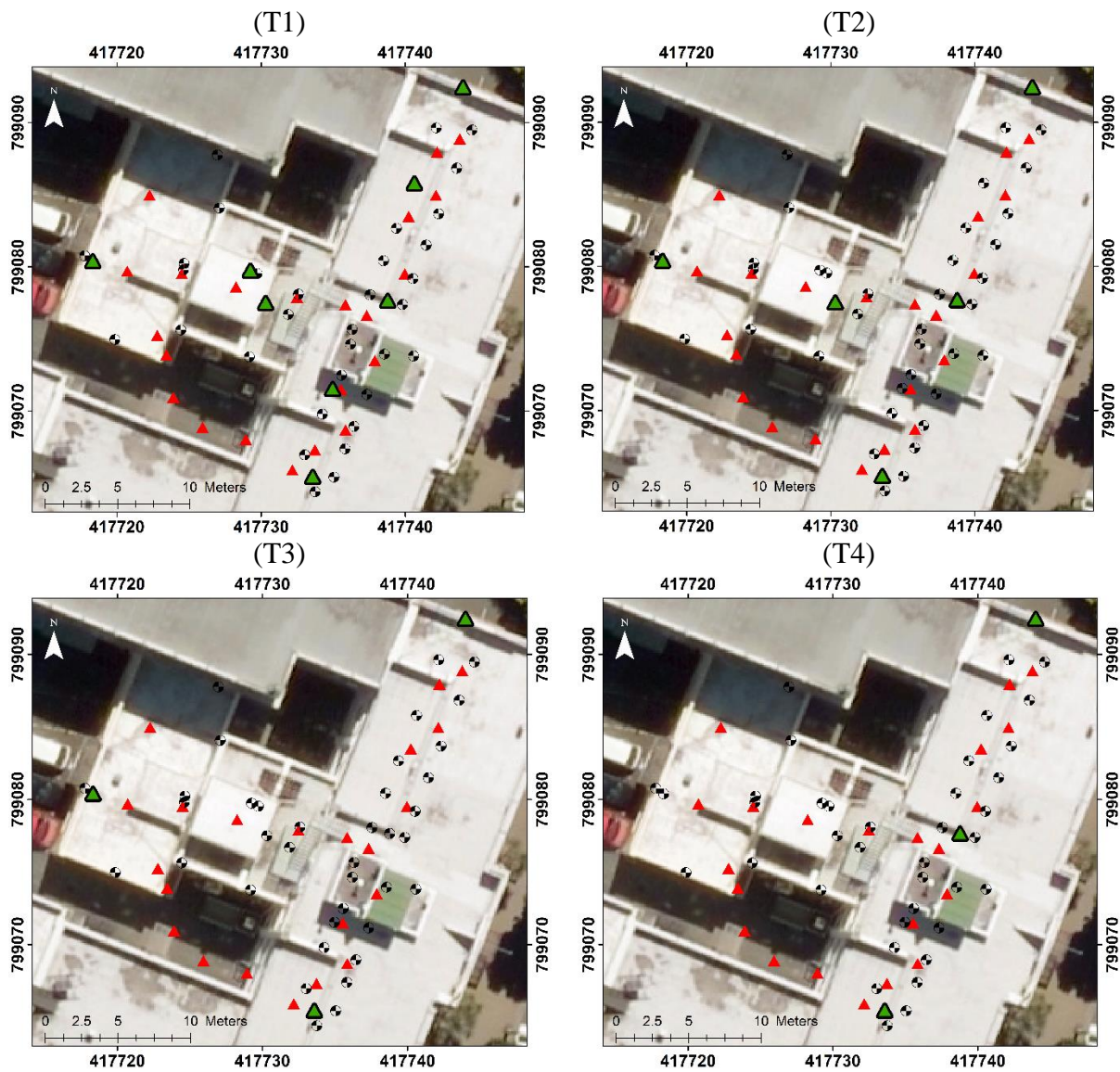
## 3.2 School of Surveying TLS Survey and Processing

A TLS survey was performed using the Trimble TX5 laser scanner, completing a total of 23 scans (Figure 1). The instrument resolution was set at 12mm @ 30m, with many surfaces scanned being closer than 10m. RealWorks v10.0 was used for the processing of the scan data. For consistency when undertaking the SoS accuracy assessment of various georeferencing scenarios, as well as this being the registration technique applicable to the LiDARRAS project, the data was registered using surface to surface registration techniques.

A reference scenario, T1, was defined to which other georeferencing scenarios were compared. T1 included eight Ground Control Points (GCPs) spread throughout and around the scan scene. Other tested scenarios include five GCPs (T2) and three GCPs (T3) spread out across the scan scene, three GCPs (T4) configured as a baseline, and three GCPs (T5) grouped to a single side of the scan scene (Figure 2).

After each adjustment scenario, RealWorks output a report for each station documenting a translation vector, Euler rotation vector, and corresponding angle of rotation relative to each station's IRS. For each scenario, these transformation parameters were reduced to the origin of the

first station and their departure from the T1 scenario analysed. Each remaining target was used as a Check Point (CP) to assess the accuracy of the point cloud data under the above georeferencing scenarios.
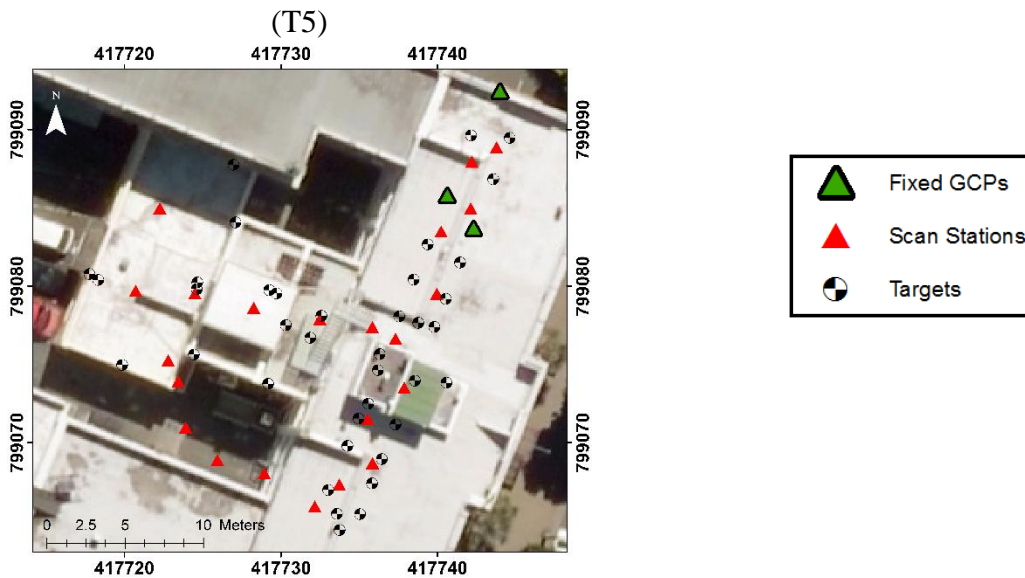
**Figure 2. Various test scenario GCP configurations. The reference scenario being T1.**

## 4. RESULTS AND DISCUSSION

### 4.1 Survey of the reference network

Results of the least squares adjustment for the CPs are shown in Table 2. The largest error at the 95% confidence interval for a single CP (0001) is 0.011m in the horizontal plane (Table 2). A single total station observation made to point 0001 when establishing the coordinates could be a possible reason for the larger error. The errors for the other CPs are close to 0.003m.

**Table 2. Horizontal and Vertical errors at the 95% Confidence Interval for the test check points.**

| Point ID | Hor.Err (m) @ 95% C.I | Vrt.Err (m) @ 95% C.I | Point ID | Hor.Err (m) @ 95% C.I | Vrt.Err (m) @ 95% C.I |
|---|---|---|---|---|---|
| **0001** | 0.011 | 0.001 | **0019** | 0.005 | 0.001 |
| **0002** | 0.001 | 0.000 | **0020** | 0.002 | 0.001 |
| **0003** | 0.002 | 0.001 | **0021** | 0.004 | 0.001 |
| **0004** | 0.002 | 0.001 | **0022** | 0.002 | 0.001 |
| **0005** | 0.004 | 0.001 | **0023** | 0.003 | 0.001 |
| **0006** | 0.008 | 0.000 | **0024** | 0.002 | 0.001 |
| **0007** | 0.006 | 0.002 | **0025** | 0.004 | 0.001 |
| **0008** | 0.001 | 0.001 | **0026** | 0.002 | 0.001 |
| **0009** | 0.005 | 0.001 | **0027** | 0.002 | 0.001 |

| | | | | | |
|---|---|---|---|---|---|
| **0010** | 0.002 | 0.001 | **0028** | 0.004 | 0.001 |
| **0011** | 0.002 | 0.001 | **0029** | 0.006 | 0.001 |
| **0012** | 0.002 | 0.001 | **0030** | 0.007 | 0.001 |
| **0013** | 0.002 | 0.001 | **0031** | 0.002 | 0.000 |
| **0014** | 0.002 | 0.001 | **0032** | 0.002 | 0.001 |
| **0015** | 0.001 | 0.000 | **0033** | 0.002 | 0.001 |
| **0016** | 0.001 | 0.000 | **0034** | 0.008 | 0.002 |
| **0017** | 0.002 | 0.001 | **0035** | 0.002 | 0.000 |
| **0018** | 0.005 | 0.001 | **0036** | 0.003 | 0.001 |

## 4.2 School of Surveying TLS Survey, Processing, and Results

Table 3 shows the mean and standard deviation of the difference in transformation parameters (translation and rotation) for each scenario with respect to T1. Results from the assessment show that deviations from the reference scenario (T1) occur more so when there is a shift in GCP location compared to the amount of GCPs used (Table 3). The table shows scenarios T2 and T3 involve marginal departure compared to reference scenario T1 with a mean translation of stations in the order of 1mm and mean rotation of up to 5mrad. However, scenarios T4 and T5 exhibit much greater departure in horizontal and/or elevation direction, as well as substantial rotation. This demonstrates a distortion of the final model caused by poor configuration of the GCPs network. Table 4 shows the Root Mean Square Errors (RMSE's) of all 31 CPs, showing little difference between T1, T2, and T3. Each of these test scenarios share three GCPs that cover the extent of the scan scene. This suggests placing the minimum number of GCPs, three, around the scan scene may render similar results to scenarios with more control. Comparing scenarios T4 and T5 shows an increase in RMSE for the scenarios with GCPs placed in unfavourable positions. Table 5 shows the five largest individual RMSE's of a CP. All worst values originate from scenarios T4 and T5 thus supporting the significant distortion in the georeferenced models due to unsuitable placement of GCPs.

**Table 3. Mean (μ) and standard error (σ) associated with translation (rX, rY, rZ) and rotation angles (rω, rφ, rκ) with respect to each test scenario using T1 as the reference. Values for translations and rotations are shown in mm and mrad respectively.**

| | rX | | rY | | rZ | | rω | | rφ | | rκ | |
|---|---|---|---|---|---|---|---|---|---|---|---|---|
| Scenario | μ | σ | μ | σ | μ | σ | μ | σ | μ | σ | μ | σ |
| T2 | 0 | 1 | 1 | 1 | 0 | 1 | -1 | 2 | -1 | 5 | -1 | 3 |
| T3 | 0 | 1 | 1 | 1 | -1 | 1 | 0 | 0 | 1 | 1 | -2 | 3 |
| T4 | -1 | 1 | 2 | 2 | 19 | 24 | -23 | 15 | 16 | 16 | 4 | 3 |
| T5 | -8 | 15 | 9 | 11 | -1 | 8 | 5 | 3 | -6 | 5 | 36 | 31 |

Terrestrial Laser Scanning for the Documentation of Heritage Tunnels: An Error Analysis (8891)
Christopher Page, Pascal Sirguey, Richard Hemi (New Zealand), Ghyslain Ferrè, Elisabeth Simonetto, Christophe Charlet and Damien Houvet (France)

FIG Working Week 2017
Surveying the world of tomorrow - From digitalisation to augmented reality
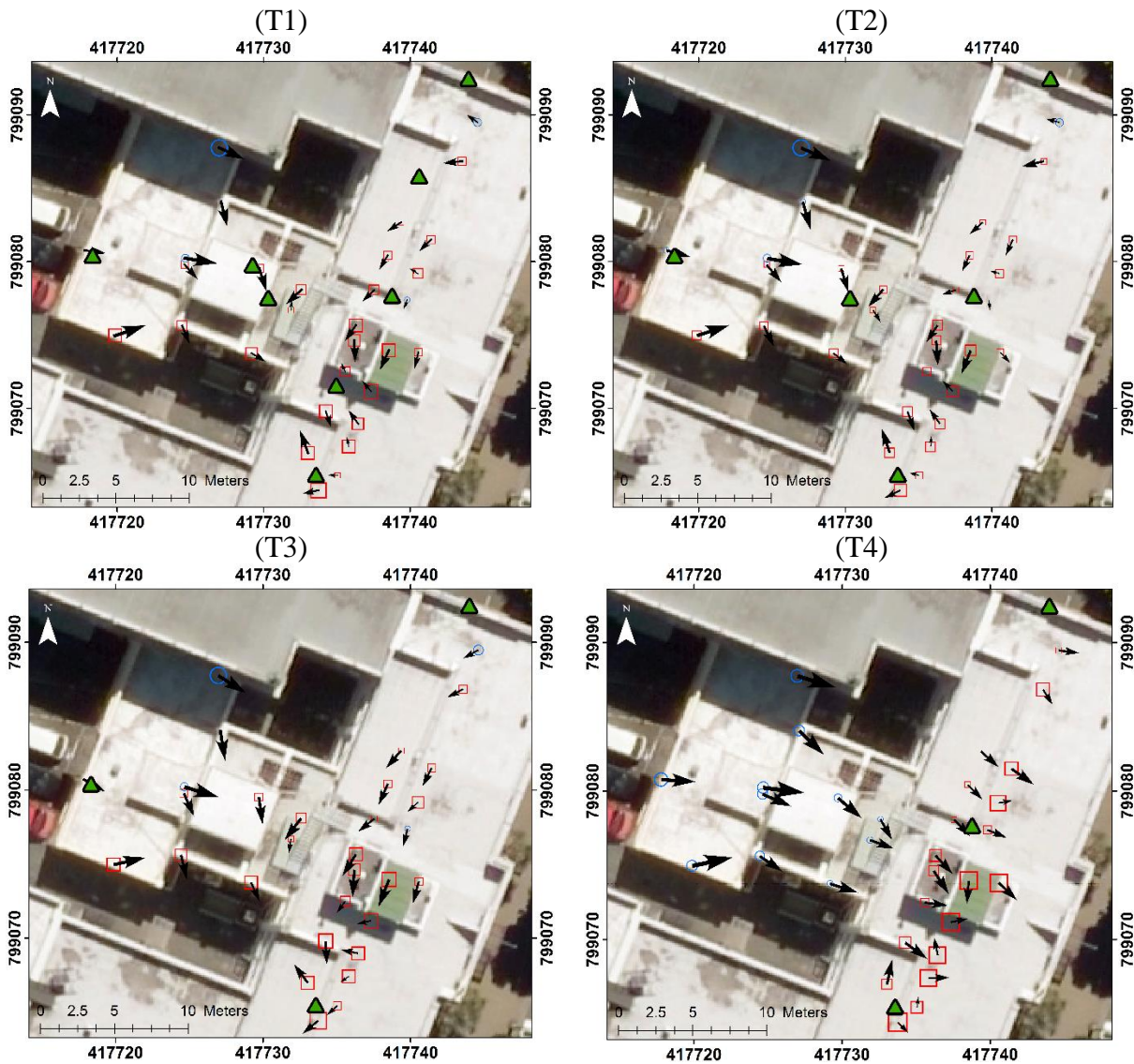Helsinki, Finland, May 29–June 2, 2017

**Table 4. Root mean square error of the 31 CPs from each scenario with respect to the reference scenario. Values are in mm.**

| Scenario | T1 | T2 | T3 | T4 | T5 |
|----------|----|----|----|----|----|
| rX | 4 | 4 | 4 | 4 | 9 |
| rY | 3 | 3 | 4 | 7 | 3 |
| rZ | 4 | 4 | 4 | 14 | 6 |

**Table 5. Five largest individual CP root mean square errors. Values are in mm.**

| Scenario | T4 | T4 | T5 | T5 | T4 |
|----------|----|----|----|----|----|
| rX | 1 | 4 | 33 | 32 | 2 |
| rY | 11 | 14 | 1 | 6 | 16 |
| rZ | 38 | 34 | 16 | 13 | 27 |
| rXYZ | 23 | 22 | 21 | 20 | 18 |

A graphical representation of CP differences for the various scenarios is seen in Figure 3. The figures show apparent systematic errors for scenarios T4 and T5. T4 displays a shift in the horizontal plane of all CPs toward the GCP baseline, with the magnitude of these horizontal errors increasing with distance from the GCPs, a sign of increasing error propagation. The vertical plane shows a rotation from a positive to negative difference from west to east as the CPs approach the GCP baseline. T5 displays horizontal errors that rotate about the GCPs and increase in magnitude with an increase in distance from the GCPs. In the vertical plane, it appears as though similar characteristics are seen to T4 where there is a change from positive to negative differences. A possible reason for the results from T4 and T5 being the way the point cloud is adjusted during the georeferencing LS adjustment. It suggests the registered point cloud moves as a single rigid-body.

Terrestrial Laser Scanning for the Documentation of Heritage Tunnels: An Error Analysis (8891)
Christopher Page, Pascal Sirguey, Richard Hemi (New Zealand), Ghyslain Ferrè, Elisabeth Simonetto, Christophe Charlet and Damien Houvet (France)

FIG Working Week 2017
Surveying the world of tomorrow - From digitalisation to augmented reality
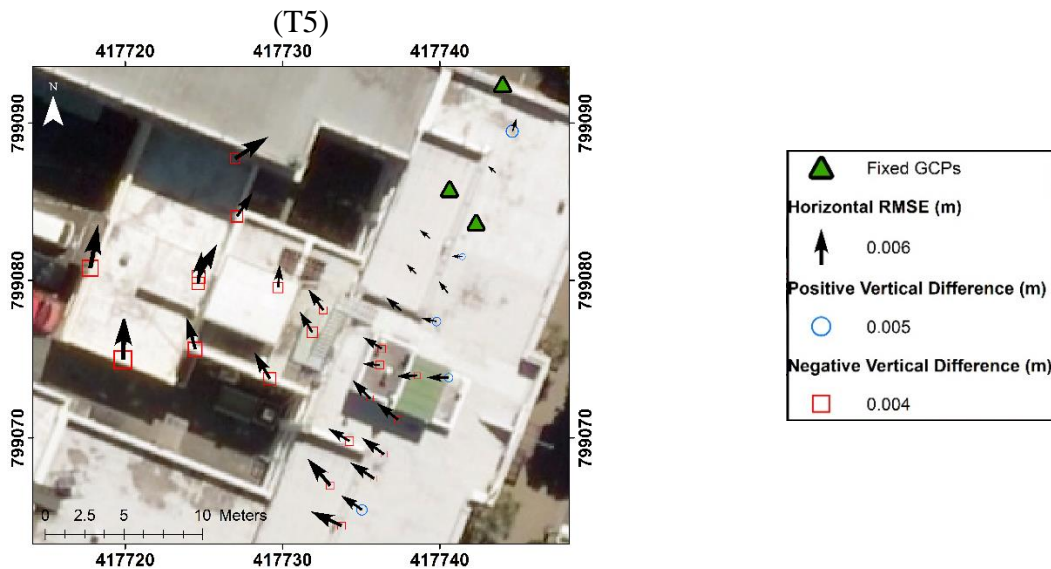Helsinki, Finland, May 29–June 2, 2017

(T1) (T2) (T3) (T4)

**Figure 3. Checkpoint root mean square errors for scenario T1 to T5. Note the systematic distortion associated with T4 and T5.**

There appears to be little difference associated with the amount of GCPs used, as long as they are placed around the scan scene, while the significant errors can be generated by unsuitable geometry of the GCPs network (Table 4). The scan scene area should be considered when deciding on the amount of GCPs used. The scan scene geometry and dataset size used in this research are favourable when georeferencing using three GCPs, scenario T3. For larger datasets, further GCPs may be required to achieve specific accuracies and limit error propagation between GCPs. This test at the SoS was necessary to better understand achievable accuracies when designing the LiDARRAS project. Things to consider about the LiDARRAS project include the magnitude of the project compared to the small test area at the SoS magnitude of scans; namely 23 were collected at the SoS while the LiDARRAS project produced close to 1,000.

## 5. LIDARRAS

### 5.1 Control Network

The control network for the LiDARRAS project was established using various traditional surveying techniques on two surveying campaigns in November 2015 and June 2016. The control network was coordinated in terms of a regional projection of the French Geodesic System RGF93; the Conformal Conic Zone 9 (CC50). GNSS was used to establish coordinates for marks above the surface of the tunnels, while the network was extended underground using a Leica TCR1201, having an angular precision of 1". The survey software adjustment program COVADIS was used to complete a LS adjustment. Figure 4 and Figure 5 show the complete underground network of the three quarries and points that were used as GCPs for the final georeferencing of the point cloud data. Each position's horizontal and vertical uncertainties are shown in
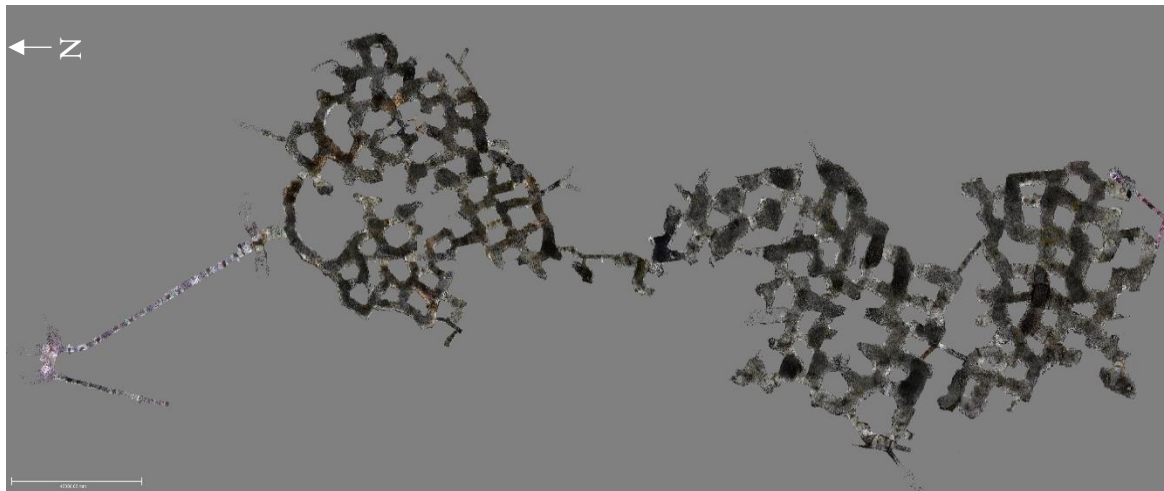
Table **6**.

**Figure 4. Point cloud showing the extent of the captured underground models. A tunnel to Wellington (left), Nelson (centre), and Blenheim (right). Note the scale bar represents 40m.**

**Table 6. The network point uncertainties at the 95% confidence interval. Positions shown as "fixed" were used to coordinate subsequent points and are assumed to have no error. Where points show "N/A" for the vertical uncertainties, no LS adjustment was computed and a 4cm misclose distributed evenly between each mark.**

| Point ID | Hor.Err (m) @ 95% C.I | Vrt.Err (m) @ 95% C.I | Point ID | Hor.Err (m) @ 95% C.I | Vrt.Err (m) @ 95% C.I |
|---|---|---|---|---|---|
| WELL01 | 0.007 | N/A | N108 | 0.020 | 0.006 |
| WELL02 | 0.004 | N/A | N109 | 0.018 | 0.006 |
| WELL03 | 0.004 | N/A | B101 | 0.014 | 0.006 |
| WELL04 | 0.004 | N/A | B102 | 0.013 | 0.006 |
| WELL05 | 0.004 | N/A | W301 | 0.002 | 0.002 |
| WELL06 | 0.004 | N/A | W302 | 0.008 | 0.004 |
| WELL07 | 0.004 | N/A | W303 | 0.008 | 0.005 |
| WELL08 | 0.004 | N/A | W304 | 0.010 | 0.005 |
| WELL09 | 0.004 | N/A | W305 | 0.013 | 0.006 |
| WELL10 | 0.004 | N/A | W306 | 0.013 | 0.006 |
| WELL11 | 0.005 | N/A | W307 | 0.014 | 0.006 |
| WELL12 | 0.005 | N/A | W308 | 0.014 | 0.006 |
| WELL13 | 0.006 | N/A | W309 | 0.016 | 0.006 |
| WELL14 | 0.006 | N/A | W310 | 0.017 | 0.006 |
| WELL15 | 0.008 | N/A | W311 | 0.019 | 0.006 |
| WELL16 | 0.009 | N/A | W312 | 0.018 | 0.006 |
| WELL17 | 0.009 | N/A | W313 | 0.018 | 0.006 |
| WELLGPS1 | Fixed | Fixed | W314 | 0.017 | 0.006 |
| WELLGPS2 | Fixed | Fixed | W315 | 0.016 | 0.005 |
| WELLGPS3 | Fixed | Fixed | W316 | 0.014 | 0.005 |
| N102 | 0.017 | 0.006 | W317 | 0.013 | 0.004 |
| N103 | 0.018 | 0.006 | W318 | 0.012 | 0.004 |

| | | | | | |
|---|---|---|---|---|---|
| N104 | 0.017 | 0.006 | **W319** | 0.008 | 0.003 |
| N105 | 0.021 | 0.007 | **W320** | Fixed | Fixed |
| N106 | 0.022 | 0.007 | **W102** | | |
| N107 | 0.020 | 0.007 | **W106** | | |

## 5.2 LiDARRAS TLS Survey, Processing, and Results

The TLS data was captured using the Trimble TX8 and the Trimble TX5. The TX5 was used predominantly in areas where the distance between the scanner and the surface was less than 0.6m as the TX8 does not return a reliable signal at such short range. These areas consisted mostly of tunnel exits. Overall, 967 scans were completed to capture the quarries of Wellington, Nelson, and Blenheim, which were processed using Trimble RealWorks v 10.1. Figure 5 shows 22 sphere markers used as GCPs to complete the georeferencing of the underground quarries.



**Figure 5. Series of GCPs that have been used for the georeferencing of the point cloud data. Axes represent planimetric coordinates in meters.**

Ground control was placed in such a way that it optimised spatial coverage around the scan scene as informed by test at the SoS. The RMSE for each GCP after georeferencing is shown in Table 7, and a visual representation of the departure between the coordinated ground control and the LS georeferencing adjustment is shown in Figure 5 and Figure 6. One must consider the uncertainty in the error of each coordinated point when analysing the accuracy of the LS adjustment, where the largest RMSE for a position being 27mm for W316 in the horizontal plane and 28mm for N109 in the vertical plane. The overall adjustment yielded an RMSE of 12mm and 9mm in the horizontal and vertical planes respectively.

**Table 7. Coordinate RMSE after the georeferencing LSE adjustment. Values are in mm.**

| Station | rX | rY | rZ |
|---|---|---|---|
| **W320** | 0.005 | 0.002 | 0.006 |
| **B102** | 0.002 | 0.001 | 0.007 |
| **W319** | 0.004 | 0.008 | 0.005 |
| **B101** | 0.006 | 0.009 | 0.008 |
| **N103** | 0.002 | 0.010 | 0.017 |
| **W318** | 0.008 | 0.003 | 0.007 |
| **W317** | 0.002 | 0.001 | 0.009 |
| **W316** | 0.019 | 0.018 | 0.015 |
| **N102** | 0.019 | 0.013 | 0.012 |
| **W313** | 0.008 | 0.008 | 0.002 |
| **N105** | 0.006 | 0.001 | 0.008 |
| **N109** | 0.009 | 0.003 | 0.028 |
| **N107** | 0.008 | 0.000 | 0.003 |
| **W309** | 0.008 | 0.005 | 0.007 |
| **W308** | 0.013 | 0.003 | 0.001 |
| **W306** | 0.023 | 0.012 | 0.006 |
| **W305** | 0.022 | 0.002 | 0.009 |
| **W302** | 0.024 | 0.009 | 0.001 |
| **W102** | 0.003 | 0.006 | 0.002 |
| **W106** | 0.002 | 0.006 | 0.003 |
| **W110** | 0.004 | 0.005 | 0.003 |
| **W113** | 0.003 | 0.015 | 0.006 |

A comparison was made between an overall adjustment whereby the entire point cloud was georeferenced as a single entity and the individual quarries being georeferenced separately. To signify the importance of spatial coverage of GCPs a comparison was made with only three GCPs being held fixed. The RMSE result for this comparison is shown in Table 8. There are no significant differences between the RMSE values when using all GCPs or georeferencing quarries individually.

A significant difference is seen in when only three GCPs are held fixed (Figure 7). Interestingly, the RMSE in the vertical component remains under 10mm. This is possibly due to the TLS instrument's dual-axis compensator being enabled during the data collection process. The horizontal displacement for this scenario shows significant error compared to the other two scenarios. This adjustment shows similarities to the School of Surveying test scenario T5 (Figure 3) where an increase in range from fixed control induces an increase in RMSE. The largest RMSE being the point furthest away, having a departure of 0.456m from the survey network position. Consideration should be given to the range at which scanning occurs from the GCPs in order to maintain point cloud accuracy.

**Table 8. Root mean square errors for the various georeferencing scenarios. Values are in mm.**

| Scenario | All | Wellington | Nelson | Blenheim | Blenheim 3 GCPs Fixed |
|---|---|---|---|---|---|
| rX | 12 | 15 | 12 | 9 | 102 |
| rY | 8 | 8 | 10 | 8 | 70 |
| rZ | 10 | 5 | 12 | 9 | 9 |
| rXYZ | 17 | 17 | 20 | 15 | 124 |

The horizontal RMSE differences (Figure 6) show a similar magnitude and direction between adjustments. Georeferencing each quarry individually bears no immediate benefit with respect to the final RMSE of each point. Individual point clouds were sampled at 2mm subsequent to registration and georeferencing. 2mm was chosen due to the nature of the surfaces being surveyed, with intricate details requiring recording while keeping the size of the dataset manageable. The three underground quarries (Figure 4) represent a combined point cloud size of approximately 20 billion points.

Terrestrial Laser Scanning for the Documentation of Heritage Tunnels: An Error Analysis (8891)
Christopher Page, Pascal Sirguey, Richard Hemi (New Zealand), Ghyslain Ferrè, Elisabeth Simonetto, Christophe Charlet and Damien Houvet (France)

FIG Working Week 2017
Surveying the world of tomorrow - From digitalisation to augmented reality
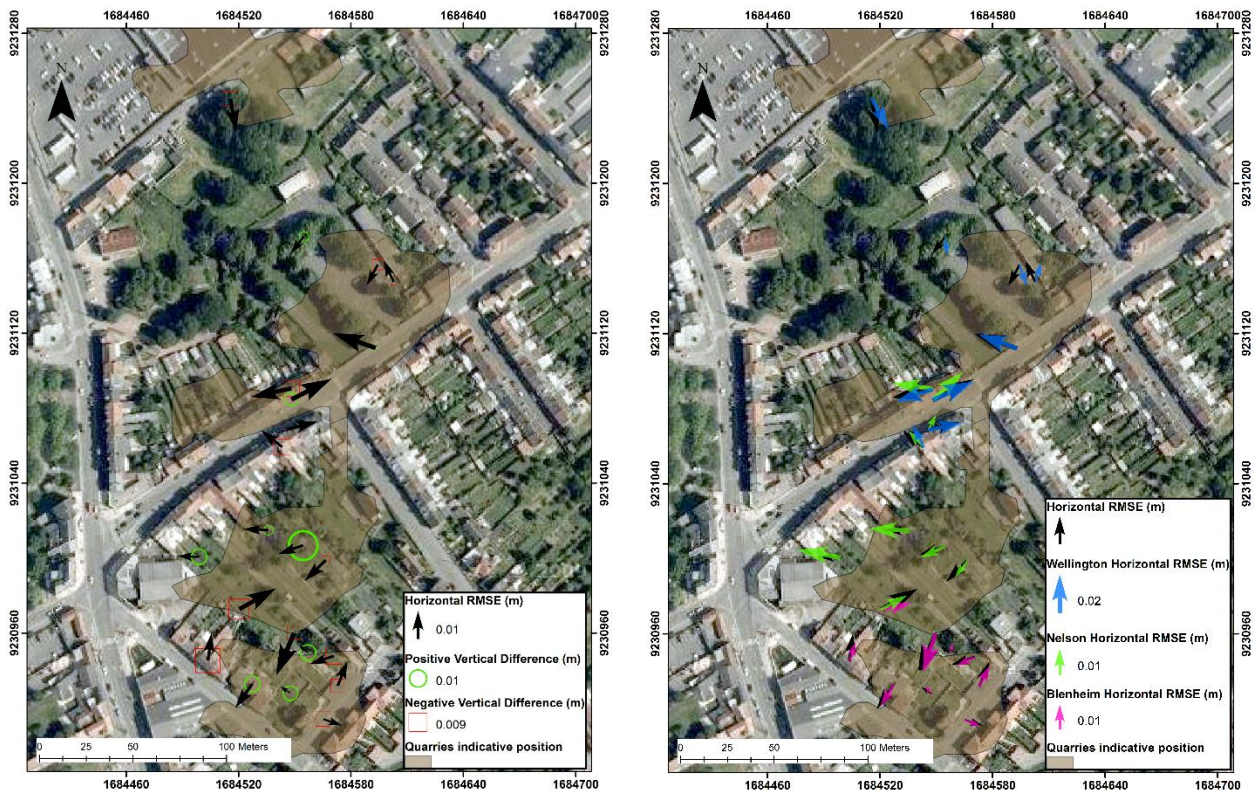Helsinki, Finland, May 29–June 2, 2017

**Figure 6. Positional differences between the total station and the TLS coordinates. (right) The total station coordinates have been used as the known coordinates. A horizontal comparison between completing the georeferencing for the entire project point cloud (black) against georeferencing each quarry individually.**

Terrestrial Laser Scanning for the Documentation of Heritage Tunnels: An Error Analysis (8891)
Christopher Page, Pascal Sirguey, Richard Hemi (New Zealand), Ghyslain Ferrè, Elisabeth Simonetto, Christophe Charlet and Damien Houvet (France)

FIG Working Week 2017
Surveying the world of tomorrow - From digitalisation to augmented reality
Helsinki, Finland, May 29–June 2, 2017

**Figure 7. RMSE when only three GCPs are held fixed. Showing significant horizontal error with an increase in range from the held GCPs.**

## 6. CONCLUSSION AND FUTURE WORK

In this contribution various GCP scenarios to georeferenced TLS point cloud were analysed where the placement and number of GCPs were altered. It was shown that the placement of ground control over the quantity used could render better results. An even spatial coverage around the scan scene supports reduced coordinate error during the georeferencing LSE adjustment. The project objective to survey and document the tunnels has been achieved with an overall RMSE of 0.03m. This was achieved by covering, where possible, the extent of the scan scene with GCPs utilising the capabilities of various surveying techniques. Quarries were registered and georeferenced individually and together as a single entity with little difference shown in the RMSE. With an accurate georeferenced point cloud, a subsequent step using the data could be to create deliverables that can be made available to the public through online platforms in an attempt to preserve and create a lasting record of the remaining Ronville Tunnels.

## 7. ACKNOWLEDGEMENTS

## 8. REFERENCES

Alba M, Scaioni M, (2007). "Comparison of techniques for terrestrial laser scanning data georeferencing applied to 3-D modelling of cultural heritage." *The International Archives of the Photogrammetry, Remote Sensing and Spatial Information Sciences* 36(5/W47): 8.

Bae K H, and Lichti D D, (2008). "A method for automated registration of unorganised point clouds." *ISPRS Journal of Photogrammetry and Remote Sensing* 63(1): 36-54.

Becerik-Gerber B, Jazizadeh F, Kavulya G, Calis G, (2011). "Assessment of target types and layouts in 3D laser scanning for registration accuracy." *Automation in Construction* 20(5): 649-65

Bornaz L, Lingua A, Rinaudo F, (2002). "Engineering and environmental applications of laser scanner techniques." *International Archives of Photogrammetry, Remote Sensing and Spatial Information Sciences* 34(3/B): 40-43.

Bornaz L, Lingua A, Rinaudo F, (2003). "Multiple scanner registration in LIDAR close-range applications." *International Archives of Photogrammetry, Remote Sensing and Spatial Information Sciences* 34(5/W12): 72-77.

Chen Y, Medioni G, (1992). "Object modelling by registration of multiple range images." *Image and vision computing* 10(3): 145-155.

Fan L, Smethurst J A, Atkinson P M, and Powrie W, (2015). "Error in target-based georeferencing and registration in terrestrial laser scanning." *Computers & Geosciences.* 83: 54-64.

Lichti D D, Gordon S, Tipdecho T, (2005). "Error Models and Propagation in Directly Georeferenced Terrestrial Laser Scanner Networks." *Journal of Surveying Engineering* 131(4): 135-142.

Lichti D D, and Skaloud J, (2010). Registration and Calibration. In *Airborne and Terrestrial Laser Scanning*, G. Vosselman and H.-G. Maas (Eds.). Whittles Publishing: Caithness, UK, 83-133.

Terrestrial Laser Scanning for the Documentation of Heritage Tunnels: An Error Analysis (8891)
Christopher Page, Pascal Sirguey, Richard Hemi (New Zealand), Ghyslain Ferrè, Elisabeth Simonetto, Christophe Charlet and Damien Houvet (France)

FIG Working Week 2017
Surveying the world of tomorrow - From digitalisation to augmented reality
Helsinki, Finland, May 29–June 2, 2017

Nettley A, Anderson K, DeSilvey C, Caseldine C, (2011). "Using Terrestrial Laser Scanning and LiDAR Data for Photo-realistic Visualization of Climate Impacts at Heritage Sites." *International Archives of Photogrammetry, Remote Sensing and Spatial Information Sciences* 38: 5.

Nuttens T, De Wulf A, Bral L, De Wit B, Carlier L, De Ryck M, Stal C, Constales D, De Backer H, (2010). "High resolution terrestrial laser scanning for tunnel deformation measurements". FIG Congress.

Paffenholz J A, Alkhatib H, Kutterer H, (2010). "Direct geo-referencing of a static terrestrial laser scanner." *Journal of Applied Geodesy* 4(3): 115-126.

Pejić M, (2013). "Design and optimisation of laser scanning for tunnels geometry inspection." *Tunnelling and Underground Space Technology* 37: 199-206.

Remondino F, (2011). "Heritage recording and 3D Modelling with Photogrammetry and 3D Scanning." *Remote Sensing* 3(6): 1104-1138.

Reshetyuk Y, (2009). "Self-calibration and direct georeferencing in terrestrial laser scanning." Doctoral Thesis, KTH.

Reshetyuk Y, (2010). "Direct georeferencing with GPS in terrestrial laser scanning." *Z f V-Zeitschrift für Geodäsie, Geoinformation und Landmanagement* 135(3): 151-159.

Rodríguez-Gonzálvez P, Nocerino E, Menna F, Minto S, Remondinob F, (2015). "3D Surveying & Modelling of Underground Passages in WWI Fortifications." *ISPRS-International Archives of the Photogrammetry, Remote Sensing and Spatial Information Sciences* 1: 17-24.

Theiler P W, Schindler K, (2012). "Automatic Registration of Terrestrial Laser Scanner Point Clouds Using Natural Planar Surfaces." *ISPRS Annals of the Photogrammetry, Remote Sensing and Spatial Information Sciences.* I-3: 173-178.

**CONTACTS**

Mr Christopher Page
The University of Otago, National School of Surveying
310 Castle Street
Dunedin
NEW ZEALAND
Tel. +64 (0)3 479 7585
Fax + 64 (0)3 479 7586
Email: pagch909@student.otago.ac.nz
http://www.otago.ac.nz/lidarras/index.html

Terrestrial Laser Scanning for the Documentation of Heritage Tunnels: An Error Analysis (8891)
Christopher Page, Pascal Sirguey, Richard Hemi (New Zealand), Ghyslain Ferrè, Elisabeth Simonetto, Christophe Charlet and Damien Houvet (France)

FIG Working Week 2017
Surveying the world of tomorrow - From digitalisation to augmented reality
Helsinki, Finland, May 29–June 2, 2017